JOURNAL OF Materials CHEMISTRY

Structural study of two layered phases in the $Na_xMn_yO_2$ system. Electrochemical behavior of their lithium substituted derivatives

Laure Bordet-Le Guenne,[a] Philippe Deniard,*[a] Philippe Biensan,[b] Clémence Siret[b] and Raymond Brec[a]

[a]*Laboratoire de Chimie des Solides, IMN, 2 rue de la Houssinière, B.P. 32229, 44322 Nantes cedex 3, France*
[b]*SAFT, 111-113 Bd A. Daney, 33074 Bordeaux, France*

Received 8th June 2000, Accepted 23rd June 2000
Published on the Web 10th August 2000

Two manganese oxide phases, α-$Na_{0.51}Mn_{0.93}O_2$ and β-$Na_{0.52}MnO_2$, have been synthesized and their structures determined by Rietveld analysis: α-$Na_{0.51}Mn_{0.93}O_2$ (isostructural to $NaCo_2O_4$) space group $P6_3/mmc$, $a=2.8661(4)$ Å, $c=11.165(4)$ Å and β-$Na_{0.52}MnO_2$ (isostructural to α-$K_{0.51}Mn_{0.93}O_2$), space group $Cmcm$, $a=2.834(6)$ Å, $b=5.216(1)$ Å and $c=11.280(3)$ Å. Both phases are layered, with alternate sheets comprised of (MnO_6) octahedra and (NaO_6) trigonal prisms. Ion exchange of Na for Li in a sample having the mean composition $Na_{0.56}Mn_{0.86}O_2$ that represents a 1 : 3 mixture of the α- and β-phases, was effected by immersion in an LiCl/$LiNO_3$ eutectic to obtain the lithiated composition $Li_{0.54}Na_{0.02}Mn_{0.86}O_2$. The latter material displayed excellent electrochemical behavior when employed as a cathode in a lithium battery. A high and relatively stable capacity of 160 mA g^{-1} was obtained in the 2.5–4.3 V voltage window for a C/15 regime. No transition to a spinel structure occurred, on cycling: the discharge/charge curves showed only a monotonous potential variation even after 50 cycles.

I Introduction

Recently, new synthesis procedures have been applied to the preparation of novel manganese oxide phases.[1,2] Following on from this work, we have investigated the synthesis of new lithium and manganese oxide materials for battery applications by substitution of lithium for sodium in $Na_xMn_yO_2$ phases that have structural features favorable for cationic mobility. Some phases in the Li–Mn–O system have already been reported to have good cathode characteristics, such as m-$LiMnO_2$[2] and o-$LiMnO_2$[3] in addition, of course, to the extensively and intensively studied $LiMn_2O_4$ spinel compounds and their transition metal substituted derivatives.[4,5,6,7]

The $Na_xMn_yO_2$ phases can be classified into two main groups with three-dimensional (3D) and two-dimensional (2D) structures comprised of tunnels or layers, respectively, that house the alkali-metal. In the case of the layered phases, these layers are exclusively built of [MnO_6] octahedra. All the Na_xMnO_2 phases with a low sodium content have 3D structures whereas for the higher sodium concentration, 2D arrangements are found. Fig. 1 gives the composition and the structure types known at present in the $Na_xMn_yO_2$ system ($x \leqslant 1$).[8]

We engaged in studies on layered compounds because of their very favorable features for fast lithium diffusion. A particularly interesting system for investigation is $Na_{0.70}MnO_{2+y}$. Earlier studies reported that these phases were of the stoichiometry $Na_{0.70x}MnO_{2+y}$, but since there is no "over-stoichiometry" in the materials but rather manganese deficiency, it is more fitting to formulate them as: $Na_{0.70(1+(y/2))}Mn_{1/(1+(y/2))}O_2$. More simply, the formulation $Na_{0.70x}Mn_xO_2$ with $x=1/(1+y/2)=2/(2+y)$ is preferred (however, as far as chemical composition is concerned, see below).

Two layered 2D allotropic phases, α and β[9] were reported for $Na_{0.70x}Mn_xO_2$ (Fig. 1(d), (e)), although no structural work has been mentioned to substantiate that claim. These two forms were said to correspond to two composition domains with a hexagonal and orthorhombic symmetry for the α and β form respectively. The oxygen-rich stoichiometry α-$Na_{0.70}MnO_{2+y}$ was reported to occur in the range $0.05<y<0.25$ and β-$Na_{0.70}MnO_{2+y}$ for $y<0.05$. For a $Na_{0.70x}Mn_xO_2$ formulation

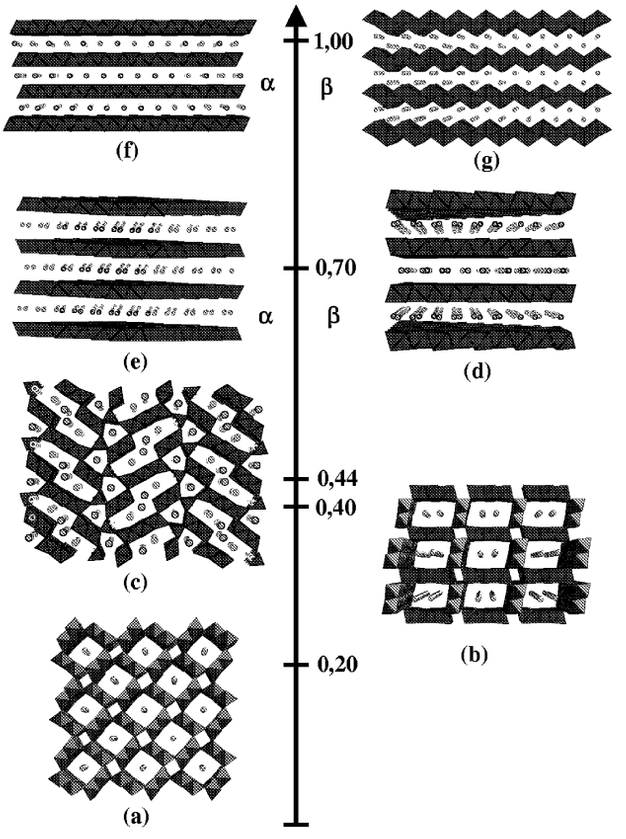

Fig. 1 Structure of the $Na_xMn_yO_2$ compounds *vs.* the Na/Mn ratio showing the 3D to 2D transition.

DOI: 10.1039/b004598p

expressed in terms of a manganese deficiency, the α and β domains correspond to $Na_{0.62}Mn_{0.89}O_2/Na_{0.68}Mn_{0.975}O_2$ and $Na_{0.68}Mn_{0.975}O_2/Na_{0.70}MnO_2$, respectively. In addition, intercalation/deintercalation electrochemical experiments[10] have shown that there exists a solid solution domain for the composition range $0.45 \leqslant x \leqslant 0.85$ with conservation of the pristine structure that is in accord with a topotactic reaction. This indeed demonstrates that the α- and β-phases have structures quite favorable for reversible room temperature cation diffusion and that following lithiation of these phases, the new materials should be very good candidates as cathodic materials for lithium batteries, assuming of course that the 2D features of the lithiated derivatives are maintained. We show here, that this is indeed the case. During the preparation of this manuscript, two papers were published[11,12] on the structures and electrochemical cycling of sodium derivatives and their partially and fully lithiated phases. These results are compared to ours herein.

II Experimental

II 1: Synthesis of the $Na_xMn_yO_2$ compounds

The synthesis of the $Na_{0.70x}Mn_xO_2$ phases was effected by the high temperature reaction of Mn_2O_3 (obtained by reduction of MnO_2 (electrolyte manganese dioxide from IBA) and Na_2CO_3 (Prolabo, kept in a moisture-free environment) in a silico-aluminate boat in air. The two reactants were taken in the proportion Na/Mn = 0.72. The reaction expected for $x = 1$ is:

$$0.70Na_2CO_3 + Mn_2O_3 + 0.15O_2 \rightarrow 2Na_{0.70}MnO_2 + 0.70CO_2\uparrow$$

The structural transition of α-$Na_{0.70x}Mn_xO_2$ into β-$Na_{0.70x}Mn_xO_2$ is reported in the literature to take place above 600 °C.[9] Monitoring the X-ray diffraction diagrams of samples containing mostly α-$Na_{0.70x}Mn_xO_2$ as a function of temperature upon heat treatment at 620 °C in air confirmed the transformation into β-$Na_{0.70x}Mn_xO_2$. This reaction appears to be kinetically limited, however, as incomplete transformation occurred unless the heating rates were exceptionally low. We found that single phases of either composition were difficult to prepare owing to their composition proximity, and unnecessary from an electrochemical point of view (*vide infra*).

Samples containing a high proportion of α-$Na_{0.70x}Mn_xO_2$ (≈80%) could be obtained by heating the above mixture at 615 °C for 15 h (180 °C h^{-1}), followed by cooling to room temperature at a rate of 100 °C per hour. To form relatively pure β-$Na_{0.70x}Mn_xO_2$, the same procedure was used except that the reaction temperature was maintained at 900 °C and the sample was quenched in air after reaction. Synthesis at an intermediate temperature (800 °C for 15 h) yielded a sample that was a 1 : 3 mixture of α and β, as determined by Rietveld analysis of the XRD patterns, with a mean composition corresponding to $Na_{0.56}Mn_{0.86}O_2$. We found this phase mixture was optimum with respect to its electrochemical properties. We note that (as our XRD analysis shows — *vide infra*), the α- and β-phases differ only slightly in composition and have the same layer stacking. Importantly, phase purity is not essential for optimum electrochemical performance, as we determined by examining the performance of a range of α/β mixtures. The 1 : 3 phase mixture, henceforth called α/β-$Na_{0.70x}Mn_xO_2$ therefore was used as our starting point for the electrochemical studies.

II 2: Synthesis of the lithium sample

Prior to use as a cathode in lithium-ion batteries, it is important to exchange the Na for Li. Na/Li substitution of the $Na_{0.56}Mn_{0.86}O_2$ sample was made by heating α/β-$Na_{0.70x}Mn_xO_2$ in a large excess (×10) of the eutectic LiCl/$LiNO_3$ (×10) at the melt temperature, 270 °C. After 15 h, the flux was eliminated by washing the solid with pure, dry ethanol. The expected reaction can be written:

$$Na_{0.56}Mn_{0.86}O_2 + 10[0.12LiCl/0.88LiNO_3] \rightarrow Li_{0.56}Mn_{0.86}O_2 + 9.44[0.12LiCl/0.88LiNO_3] + 0.56[0.12LiCl/0.88NaNO_3]$$

II 3: Experimental techniques

Carbon analysis was performed by coulometric titration of CO_2 formed during the heating of the materials at high temperature under an oxygen flow. The oxygen content of the samples was obtained through firing of the samples at high temperature in a gas-free graphite boat, the CO formed being analyzed by infrared spectroscopy. The Fe, Mn, Li, Na, Ca and Mg element concentrations were determined by plasma emission spectroscopy.

X-Ray diffraction diagrams (40 kV × 30 mA) were recorded in θ–θ Bragg–Brentano geometry using a Siemens D5000 diffractometer (CuK_α-radiation) and a nickel filter. A linear Elphys detector was used. Structure determinations were carried out using the Rietveld method, employing Fullprof[13] and GSAS[14] software. The electrochemical studies of the $Li_{0.54}Na_{0.02}Mn_{0.88}O_2$ sample (obtained from a mixture of the α/β sodium derivative, see below) were performed using coin-cell batteries from the SAFT company. They were assembled in an argon filled dry box (O_2 and $H_2O \approx 1$ ppm). The cathodes were made of 80% weight of active materials (approximately 50 mg), 7.5% soot, 7.5% graphite and 5% Teflon emulsion according to a procedure described elsewhere.[15] The anode was a disk of lithium metal ($\phi = 15$ mm). The electrolyte was made of a mixture of three solvents: PC/EC/DMC in a 1 : 1 : 3 volume proportion in which 1 M $LiPF_6$ was dissolved. The batteries were tested using a MAC PILE apparatus[16] working in the galvanostatic mode between 2.5 and 4.3 volts with a C/15 regime for 0.5 lithium (11 mA g^{-1}) and a 30 minute relaxation time between each half-cycle.

The phase densities were measured using an automatic gas pycnometer (ACCUPYC 1330).

II 4: Characterization of the two α- and β-$Na_xMn_yO_2$ phases

Note that the phase compositions for the two α- and β-phases obtained within the scope of this work (see below) differ from the composition ratio Na/Mn = 0.70 reported earlier. This indicates that our elemental composition is somewhat different from the one previously found and justifies the formulation chosen for our phases of $Na_xMn_yO_2$. This composition neither strictly adheres to the $Na_{0.70x}Mn_xO_2$ formula nor any other specific composition previously reported. In fact, there is no particular reason, neither structural nor electronic, for a non-stoichiometric phase to follow a specific composition.

II 4 1: β-$Na_{0.52}MnO_2$. The β form is discussed first since it was obtained as a pure phase, contrary to the α modification (see below). The X-ray powder diffraction diagram structure refinement was carried out assuming that the compound had the same structure as the layered orthorhombic $K_{0.51}Mn_{0.93}O_2$ material.[17] This hypothesis proved correct as convergence of the calculations and satisfactory reliability factors were achieved (see below). Refinement in the orthorhombic *Cmcm* space group yielded the following cell parameters: $a = 2.834(6)$ Å, $b = 5.216(1)$ Å, $c = 11.280(3)$ Å ($V = 166.76(6)$ Å^3). Because they were difficult to refine, the atomic displacement parameters (ADP) of the atoms were constrained to keep the values they generally show in these types of phases, that is: $B_{Na} = 2$ Å^2, $B_{Mn} = 0.8$ Å^2 and $B_O = 1$ Å^2. The reliability factors converged to $R_{WP} = 1.24\%$ and $\chi^2 = 6.33$; in accord, the difference function showed that a good fit was obtained (Fig. 2). Tables 1 and 2 summarize the refinement results. Note that the estimated standard deviation

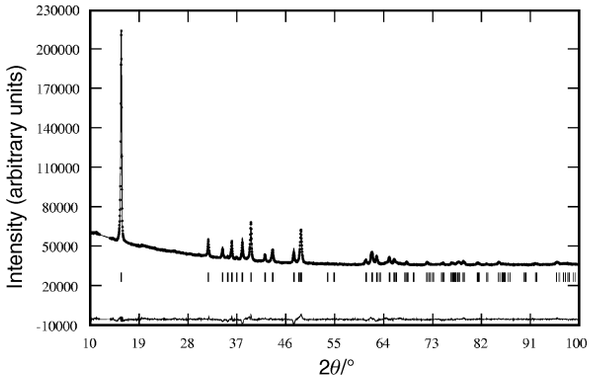

Fig. 2 Diffraction pattern of β-$Na_{0.52}MnO_2$.

values (ESDs) in Table 2 have all been multiplied by 3 to take into account the correction as suggested by J. F. Bérar[18] to avoid under-estimated ESDs. The structure, comprised of AB BA layers of oxygen designating trigonal prisms and octahedra surrounding sodium and manganese (respectively) that form alternating layers along *c* is displayed in Fig. 3.

As found by the Rietveld refinement calculations, the composition of the β-phase under study is: $Na_{0.52(2)}Mn_{0.99(1)}O_2$. The manganese concentration not being meaningfully different from 1, this justifies the title composition ($Na_{0.52}MnO_2$) that will subsequently be used in the text. This composition and the cell volume of the phase allowed us to calculate a density in good agreement with the density measured for this sample ($d_{cal}=3.916(6)$ and $d_{meas}=3.922(5)$).

A similar structural polymorph has been recently prepared by Paulsen and Dahn[12] at a temperature of 1000 °C. Some problems encountered in modeling the X-ray diffraction diagram led the authors to consider a monoclinic distortion, in which an angle of 90.68° was found. With a lower sodium content ($Na_{0.52(2)}MnO_2$ as compared to $Na_{0.66}MnO_2$), our β-phase did not show such distortion (Fig. 2), in agreement with a higher Mn^{4+} content. However, the symmetry lowering introduced in the previous report led the authors to a difference diagram that still contained some important residues. The question arises then about the true maximum sodium content that the phase can sustain. It may be that our lower sodium concentration is closer to the limit, should the residues be attributed to impurities rather than to symmetry issues.

The orthorhombic symmetry displayed by our $Na_{0.52}MnO_2$ phase may be explained by the high concentration of Mn^{3+} (mean oxidation state (O.S.) of Mn = 3.51) as opposed to the symmetry of the α-phase which is hexagonal with a mean O.S. for Mn of 3.75 (see below), *i.e.*, which contains a lower amount of Mn^{3+}. On the other hand, α-$NaMnO_2$ is even more distorted, having a monoclinic cell ($\beta=112.9°$) due to the exclusive presence of Mn^{3+}. Owing to the cooperative Jahn–

Table 1 Rietveld refinement of β-$Na_{0.52}MnO_2$. Estimated standard deviations have been multiplied by 3 (σ_{corr})

Data collection
Temperature: 20 °C
Wavelength: 1.54060 and 1.54439 Å
Angular domain: $2\theta_{min}$, 10°; $2\theta_{max}$, 110°
Step, acquisition time: 0.03° (2θ), 12 s
Space group: *Cmcm*
Number of refined parameters, number of reflections: 18, 110
Cell parameters:
$a=2.834(6)$ Å, $b=5.216(1)$ Å, $c=11.280(3)$ Å
Volume, *Z*: 166.76(6) Å^3, 4
η (pseudo-Voigt): 0.64(3)
Profile parameters (*U*,*V*,*W*): 0.1(1); 0.04(2); 0.03(1)
Reliability factors:
$R_p=0.793\%$, $R_{wp}=1.24\%$, $\chi^2=6.33$

Table 2 Atomic positions, atomic displacement parameters and site occupation fraction of β-$Na_{0.52}MnO_2$. Estimated standard deviations have been multiplied by 3 (σ_{corr})

Atom	Position	*x*	*y*	*z*	*B*/Å^2	τ^a
Na1	4c	0	−0.07(1)	1/4	2	0.209(9)
Na2	4c	0	0.661(9)	1/4	2	0.315(9)
Mn1	4a	0	0	0	0.8	0.99(1)
O1	8f	0	0.659(2)	0.9096(9)	1	1

[a]Site occupation factor.

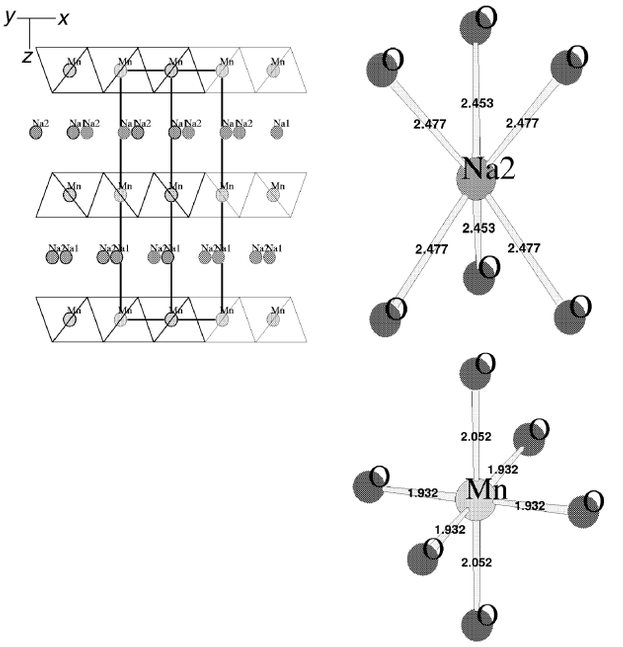

Fig. 3 The β-$Na_{0.52}MnO_2$ structure showing the Na and Mn first coordination spheres (distances in Å).

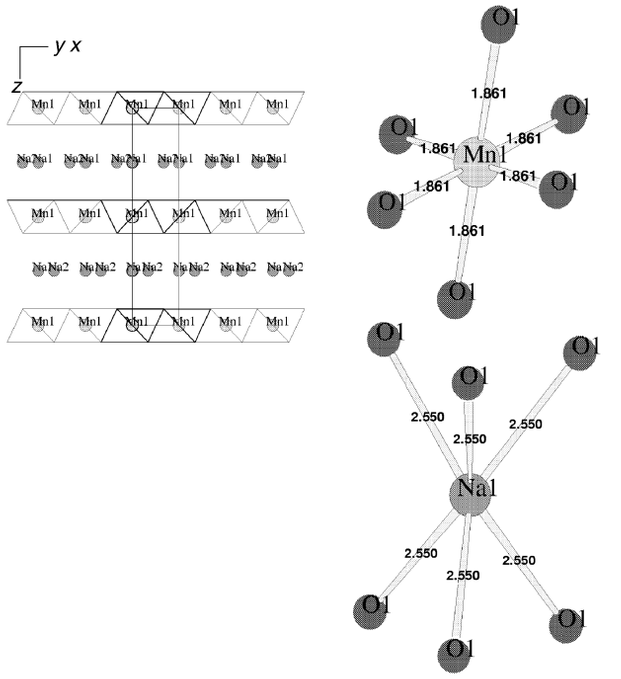

Fig. 4 The α-$Na_{0.51}Mn_{0.93}O_2$ structure showing the Na and Mn first coordination spheres (distances in Å).

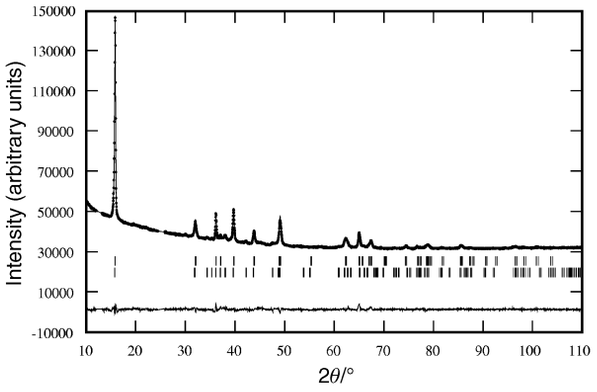

Fig. 5 Diffraction pattern of α-$Na_{0.51}Mn_{0.93}O_2$. The difference pattern shows a good agreement between calculated and observed patterns.

Teller effect, the [MnO_6] octahedra in β-$Na_{0.52}MnO_2$ are quite irregular (Fig. 4).

II 4 2: α-$Na_{0.51}Mn_{0.93}O_2$. The structure of α-$Na_{0.51}Mn_{0.93}O_2$ was assumed to be the same as that of $NaCo_2O_4$ ($P6_3/mmc$). A successful powder X-ray diffraction cell parameter refinement yielded the parameters $a=2.8661(4)$ Å, $c=11.165(4)$ Å, $V=79.42(4)$ Å^3. However, some diffraction lines could not be taken into account that were found to correspond to the β-phase. A complete structure refinement from the entire X-ray diffraction diagram was then performed, using for the α-phase the atomic coordinates of $NiCo_2O_4$ and for the β-phase the atomic coordinates found for this structure (see above). The latter values were not refined owing to the minority fraction of this phase, but the cell parameters were refined. These ones were found to be identical, within three times the ESDs values, to those found for pure β-$Na_{0.52}MnO_2$. For α-$Na_{0.51}Mn_{0.93}O_2$, as with β-$Na_{0.52}MnO_2$, the ADPs were fixed to the same typical values. The refinement was satisfactory with $R_{wp}=0.99\%$ and $\chi^2=3.41$ and a minimal difference trace (see Tables 3 and 4 for complete refinement conditions and data and Fig. 5 for the refinement diagrams). The composition of the α-$Na_{0.51}Mn_{0.93}O_2$ phase mixture was determined by refining the occupation ratio of the cation sites. This proves that the phase is not stoichiometric in manganese. Our calculations show that the sample consists of 18.5 wt% of the β-phase (a Brindley correction[19] was applied, although in this case, the X-ray absorption difference of the two phases is indeed small). The structure is composed of the same AB BA oxygen layer stacking as in the β-phase, with the same alternating layers of oxygen trigonal prisms and octahedra surrounding the sodium and manganese ions, respectively (Fig. 3). In this case however, and for the reasons explained earlier, the [MnO_6] octahedra are quite regular (Fig. 4). The synthesis of α has also been attempted recently by Paulsen and Dahn,[12] but the phase X-ray diffraction diagram proved very poor and structure refinement could not be carried out. This again may be related to the sodium content, and also perhaps to the heating conditions. It seems that slightly different temperatures may lead to completely different crystal ordering and that our synthesis conditions are closer to the ideal ones.

Table 3 Rietveld refinement of α-$Na_{0.51}Mn_{0.93}O_2$ with 18.5% of β-$Na_{0.52}MnO_2$. Estimated standard deviations have been multiplied by 3 (σ_{corr})

Data collection
Temperature: 20 °C
Wavelength: 1.54060 and 1.54439 Å
Angular range: $2\theta_{min}$, 10°; $2\theta_{max}$, 110°
Step, acquisition time: 0.03° (2θ), 12 s
α-$Na_{0.51}Mn_{0.93}O_2$
Space group: $P6_3/m$ (no. 176)
Number of refined parameters, number of reflections: 11, 104
Cell parameters: $a=2.8661(4)$ Å, $c=11.165(4)$ Å, $\gamma=120°$
Volume, Z: 79.42(4) Å^3, 2
η(pseudo-Voigt): 0.88(6)
Profile parameters (U,V,W): 0.3(1); 0.06(4); 0.02(1)
β-$Na_{0.52}MnO_2$
Space group: $Cmcm$ (no. 63)
Number of refined parameters, number of reflections: 8, 136
Cell parameters: $a=2.827(3)$ Å, $b=5.220(3)$ Å, $c=11.222(6)$ Å
Volume, Z: 165.6(3) Å^3, 4
η(pseudo-Voigt): 0.8(3)
Profile parameters (U,V,W): 0.1(1); 0.1(1); 0.01(1)
Reliability factors : $R_p=0.672\%$, $R_{wp}=0.994\%$, $\chi^2=3.41$
Weight percentages after Brindley corrections:
α-$Na_{0.51}Mn_{0.93}O_2$: 81.5, β-$Na_{0.52}MnO_2$: 18.5

Table 4 Atomic positions, atomic displacement parameters and site occupation fraction of α-$Na_{0.51}Mn_{0.93}O_2$. Estimated standard deviations have been multiplied by 3 (σ_{corr})

Atom	Position	x	y	z	B/Å^2	τ
Na1	2a	0	0	1/4	2	0.276(9)
Na2	2d	2/3	1/3	1/4	2	0.234(9)
Mn1	2b	0	0	0	0.8	0.93(1)
O1	4f	1/3	2/3	0.0762(9)	1	1

The above sample that contains substantial amounts of the β-phase as an impurity was obtained following many attempts to prepare a pure material. Synthesis temperatures below 615 °C used to avoid the formation of the unwanted impurity resulted in incomplete reactions with the occurrence of sizeable quantities of the unreacted precursors (Na_2CO_3 and Mn_2O_3).

Although the pure α-phase cannot be obtained the similar layered nature of the α- and β-phases suggests that this should not be a problem with respect to the electrochemical properties of the analogous lithium derivatives. Therefore, a sample containing both α- and β-phases in the ratio 1 : 3 was characterized, ion-exchanged by lithium and used as a cathode in a lithium battery and electrochemically cycled. As will be shown, this mixture showed remarkable electrochemical properties.

III Characterization of the $Na_xMn_yO_2$ sample used for electrochemical studies

The sample that was prepared at 800 °C contained the α- and β-phases in the ratio 25% : 75% as shown earlier. From the elemental analyses and due to the fact that these were the only phases present in the sample, the overall composition could be straightforwardly calculated as $Na_{0.56}Mn_{0.86}O_2$. This composition is lower in alkali content than previously reported compositions ($Na_{0.62}Mn_{0.89}O_2$–$Na_{0.68}Mn_{0.975}O_2$ for the α-phase and $Na_{0.68}Mn_{0.975}O_2$–$Na_{0.70}MnO_2$ for the β-phase), but our composition overlaps with that of a study reporting a lower Na/Mn ratio.[10]

Thermogravimetric studies coupled to mass spectroscopy and carried out up to 350 °C showed neither H_2O nor CO_2 loss, proving the absence of water and/or protons within the slabs of the structures, along with the absence of any other carbon-based impurities that might have escaped detection from the X-ray diffraction technique. The Rietveld diffraction pattern refinement was performed using the structural data obtained from the α and β structural parameters as determined above. No attempt was made to refine the chemical composition of the two phases. The quantities of the α- and β-phases were found to be 26% and 74% respectively. Note that the two phases react with moisture leading to the intercalation of water and to the formation of birnessite-like materials: therefore the X-ray diffraction patterns were recorded either in a dry atmosphere or in a very short time.

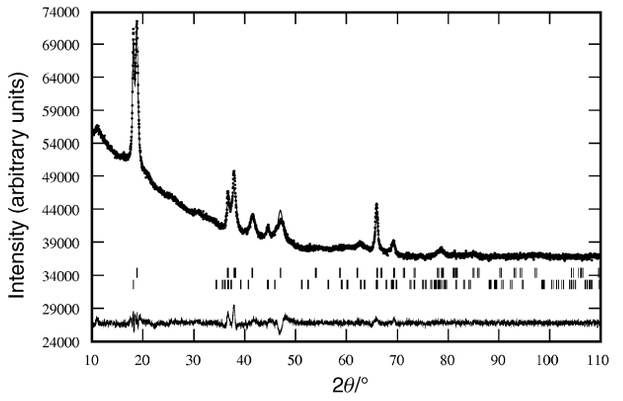

Fig. 6 $Li_{0.54}Na_{0.02}Mn_{0.88}O_2$ diffraction pattern. The refinement was performed without any structural constraint. The difference pattern indicates a very poor agreement between the observed and calculated patterns.

IV Lithium substituted phases

IV 1: Characterization

The elemental analyses led to the sample composition: $Li_{0.54}Na_{0.02}Mn_{0.86}O_2$. The amount of residual sodium is quite small ($Na/Mn \approx 0.02$) and the concentration of protons is less than 0.4%. Since the pristine sample corresponds to $Na_{0.56}Mn_{0.86}O_2$ these results show that, within deviation, there is no significant change in the manganese O.S., *i.e.* the reaction is based on simple topotactic exchange.

Fig. 6 shows the X-ray diffraction diagram of the lithiated sample. Because the initial preparation contained two phases and because the topotactic reaction was performed at a very mild temperature, it was assumed that the $Li_{0.54}Na_{0.02}Mn_{0.86}O_2$ sample also contained two similar phases. This was further confirmed by the observation that different synthetic batches contained series of the same X-ray diffraction peaks which varied in their relative intensities from sample to sample. We attempted to model the diagram with different combinations of symmetry and cell parameters without structural constraints, using TREOR and FULLPROF.[13,20] The best fit, obtained by refining only the cell parameters and the diffraction line profiles, although not completely satisfactory, is given in Fig. 6: this result corresponds to taking into account two phases with the same symmetries as those of α and β. The cell parameters found for the hexagonal phase are: ($P6_322$) $a = 2.830(1)$ Å, $b = 9.432(3)$ Å, $V = 65.44(6)$ Å^3 and for the orthorhombic phase: ($Cmcm$) $a = 2.829(3)$ Å, $b = 5.210(3)$ Å, $c = 9.784(3)$ Å and $V = 144.24(9)$ Å^3. Because of the poor fit that was obtained without structural constraints, Rietveld structure refinement was not carried out. At this stage, we propose that our phase is possibly composed of the random stacking of O2 and O4 types of layers as suggested for $Li_{0.82}Mn_{0.85}Co_{0.15}O_2$.[11] Future electron diffraction studies, however, should allow us to confirm the two-phase nature of the preparation and to confirm the symmetry suggested by the X-ray diffraction analysis.

Random stacking is not unexpected since the difference between α and β, beyond a small composition difference, originates only from a distortion. This suggests that there is no need to start from a pure (α or β) phase, since both phases will lead to the same random stacking of the O type upon full lithium substitution.

IV 2: Electrochemical studies

Figs. 7a and 7b show the charge and discharge curves of the $Li_{0.54}Na_{0.02}Mn_{0.86}O_2$/Li electrochemical system and the capacity changes as a function of cycling. The electrochemical process started with oxidation to remove residual lithium: as expected, the capacity proved very small since the O.S. of manganese is close to 4 (O.S. = 3.9). This confirmed the results of the quantitative analysis (25 mA h charge calculated for 1 g of $Li_{0.54}Na_{0.02}Mn_{0.86}O_2$ corresponds to 0.09 faraday per mole). In the voltage window 2.5–4.3 V (C/15 regime for 0.5 Li mol^{-1}), the initial capacity of 160 mA g^{-1} decreases to 140 mA g^{-1} after 50 cycles. For the same regime but in the 1.5–4.3 V potential window, a large first cycle capacity of 210 mA g^{-1} is obtained that decreases more rapidly on cycling. These first results are as promising as those recorded for *o*-$LiMnO_2$, a material patented in the past by SAFT.[21] The shapes of the electrochemical curves look very similar to those

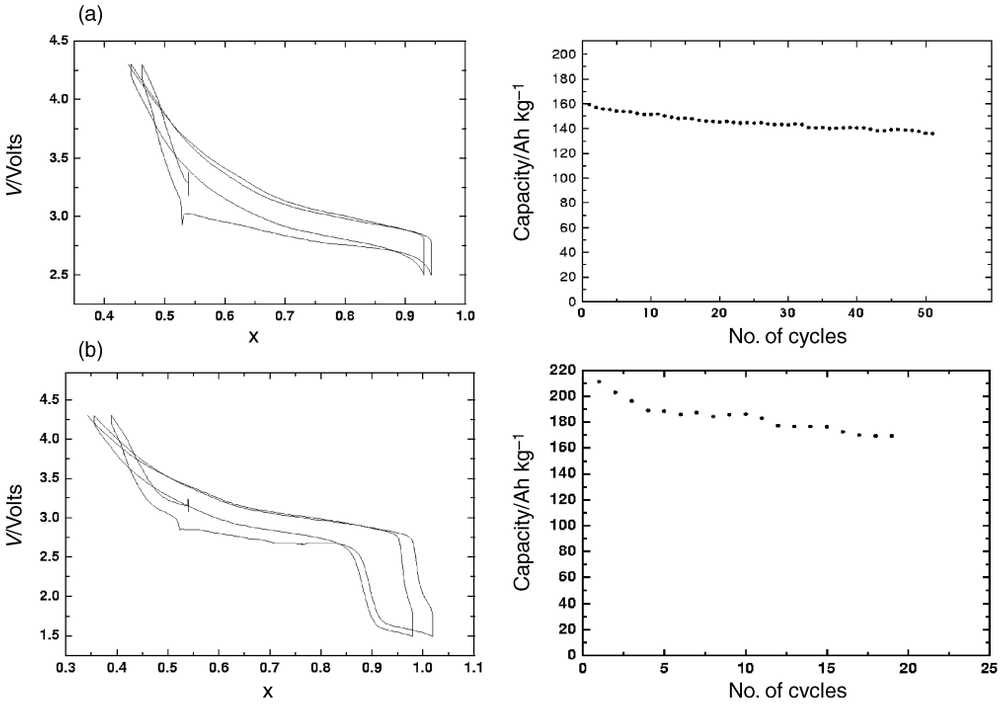

Fig. 7 $Li_{0.54}Na_{0.02}Mn_{0.88}O_2$ charge and discharge curves and electrochemical capacity *vs.* cycle number for a 2.5–4.3 V potential window (a) and a 1.5–4.3 V potential window (b).

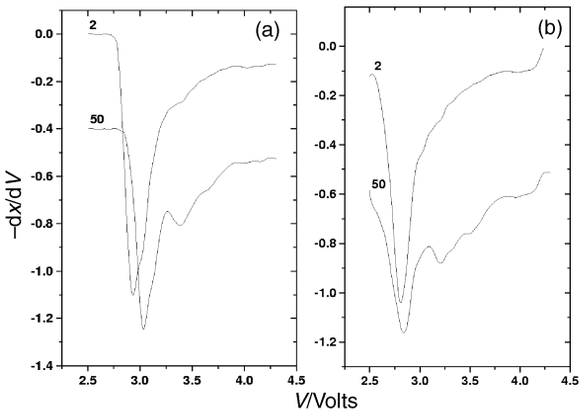

Fig. 8 Incremental capacity variation during charge (a) and discharge (b) for $Li_{0.54}Na_{0.02}Mn_{0.88}O_2$ *vs.* cycle number in a 2.5–4.3 V potential window.

of the birnessite- or rancieite-type layered phases. They are characterized in particular by a monotonous potential variation *vs.* x, that does not display an apparent transition into a spinel phase. Our results are rather different from those obtained for prelithiated $Li_{0.82}Mn_{0.84}O_2$[11] compounds, that show a small initial capacity of 55 A h kg^{-1} in the 4.4–2.0 volts range. For these compounds, the capacity can only be increased by raising the discharge cut-off to 4.6 volts, presumably as a result of some phase transition that occurs at high potential. Following this transition, the subsequent cycles show a smooth variation of potential *versus* lithium content.

As the two samples have similar composition and structure, it is difficult to understand why one sample displays a phase transition that the other one does not. However, Paulsen *et al.*[11,12] have also shown that the transition in $Li_{0.71}Mn_{0.84}O_2$ (a compound slightly different from $Li_{0.82}Mn_{0.84}O_2$ mentioned above) becomes more difficult to observe, and the capacity which begins at 120 A h kg^{-1} reaches 150 A h kg^{-1} after 10 cycles. In this particular case, the phase behavior resembles that of the sample we present here.

The absence of the two voltage plateaus of 2.9 and 4.1 volts observed in other Li–Mn–O compounds that transformed into either *in situ*-induced or were as-prepared spinel structures, is a very favorable feature of this 2D material. The absence of a phase transition towards a spinel arrangement can probably be attributed to the manganese deficiency within the lattice and also as noted previously, to the necessity to break bonds to go from an O2 to O3 oxygen stacking. Although the structure probably remains 2D as far as oxygen stacking is concerned, the Mn and Li distribution has to be 3D in order to preserve enough crystal energy stability that would prevent any (or substantial) manganese migration during cycling. Further and new structure determinations need to be made on single-phased $Li_xMn_yO_2$ samples to prove this point.

Incremental capacity curves ($dx/dV = f(V)$) in the charge and discharge regime (Fig. 8) show a peak at 2.8 V in reduction and at 2.9 V in oxidation. This small potential difference is typical of a fast and highly reversible phenomenon and is again a very positive feature for the material. On the second discharge curve, a weak, broad peak appears at 4.1 V, whose intensity remains constant upon cycling. This peak could correspond to the occurrence of a small amount of impurity initially present in the sample: an impurity that could be either some spinel or some *in situ* formed spinel stemming from a 2D $LiMnO_2$ phase. The second hypothesis seems more likely since the peak does not show up on the first cycle. After 50 cycles, a second, reversible peak appears for a potential of 3.25 V on reduction and 3.35 V on oxidation. This may be attributed to some mild structure modification not involving a transition to the spinel type.

V Conclusions

Two $Na_xMn_yO_2$ materials with two layered structures (α and β) were prepared and fully characterized. They have been found to be related to the $K_{0.51}Mn_{0.93}O_2$ (*Cmcm*) and Na_2CoO_2 ($P6_3/mmc$) phases. The correctness of the structural choice has been confirmed by the consistency of the data obtained from the chemical analyses, structurally determined compositions and density measurements. Our results have shown also that there does not seem to be any particular relation between x and y ratio of the $Na_xMn_yO_2$ samples prepared in this study, contrary to earlier reports. Sodium in $Na_xMn_yO_2$ can be easily substituted for lithium without a change in the manganese oxidation state. Electrochemically, the $Li_{0.54}Na_{0.02}Mn_{0.86}O_2$ material showed a high initial capacity of 160 mA g^{-1} in a 2.5–4.3 V potential range without optimization of the cathodic material, using the as-prepared sample. Recent results show that the final lithiated product $Li_{0.54}Na_{0.02}Mn_{0.86}O_2$ must have the same stacking fault arrangement when starting from the pure α or pure β form, indicating that the same structural transition takes place in α and β. However, prelithiation seems to have an important role in the behavior of the cathodic materials as comparisons between $Li_{0.54}Na_{0.02}Mn_{0.86}O_2$ and $Na_{0.66}MnO_2$ show and this deserves further examination.

References

1 A. R. Armstrong and P. G. Bruce, *Nature*, 1996, **381**, 499.
2 F. Capitaine, P. Gravereau and C. Delmas, *Solid State Ionics*, 1996, **89**, 3.
3 L. Croguennec, P. Deniard and R. Brec, *J. Electrochem. Soc.*, 1997, **144**, 3323.
4 M. M. Thackeray, W. I. F. David, P. G. Bruce and J. B. Goodenough, *Mater. Res. Bull.*, 1983, **18**, 461.
5 M. M. Thackeray, L. A. De Picciotto, A. De Kock, P. J. Johnson and V. A. Nicholas, *J. Power Sources*, 1987, **21**, 1.
6 M. Wohlfahrt-Mehrens, A. Butz, R. Oesten, G. Arnold, R. Hemmer and R. Huggins, *J. Power Sources*, 1997, **68**, 582.
7 C. G. Sigala, D. Verbaere, A. Piffard and Y. Tournoux, *Solid State Ionics*, 1995, **81**, 167.
8 C. Fouassier, C. Delmas and P. Hagenmuller, *Mater. Res. Bull.*, 1975, **10**, 443.
9 J. Parant, R. Olazcuaga, M. Devalette, C. Fouassier and P. Hagenmuller, *J. Solid State Chem.*, 1971, **3**, 1.
10 A. Mendiboure, C. Delmas and P. Hagenmuller, *J. Solid State Chem.*, 1985, **57**, 323.
11 J. M. Paulsen, C. L. Thomas and J. R. Dahn, *J. Electrochem. Soc.*, 1999, **146**, 3560.
12 J. M. Paulsen and J. R. Dahn, *Solid State Ionics*, 1999, **126**, 3.
13 J. Rodriguez-Carjaval, *Physica B*, 1993, **192**, 55.
14 A. C. Larson and R. B. Von Dreele, Report #LA-UR-86-748.
15 L. Croguennec, P. Deniard, R. Brec, P. Biensan and M. Broussely, *Solid State Ionics*, 1996, **89**, 127.
16 C. Mouget and Y. Chabre, *McPile*, licensed from CNRS and UJP Grenoble to BIO-LOGIC CO., 1 av. de l'Europe, 38640 Claix, France.
17 C. Delmas and C. Fouassier, *Z. Anorg. Allg. Chem.*, 1976, **420**, 184.
18 J. F. L. Bérar and P. Lelann, *J. Appl. Crystallogr.*, 1991, **24**, 1.
19 G. W. Brindley, *Philos. Mag.*, 1945, **36**, 347.
20 P. E. E. Werner, L. Eriksson and M. Westdahl, *J. Appl. Crystallogr.*, 1985, **18**, 367.
21 A. B. Lecerf and P. Baudry, Fr. Pat. Brevet FR9308484, 1993.